

Are your **MRI contrast agents** cost-effective?

Learn more about generic **Gadolinium-Based Contrast Agents**.



AJNR

**Imaging of Intra-neural Edema by Using
Gadolinium-Enhanced MR Imaging:
Experimental Compression Injury**

Shigeru Kobayashi, Adam Meir, Hisatoshi Baba, Kenzo
Uchida and Katsuhiko Hayakawa

This information is current as
of April 16, 2024.

AJNR Am J Neuroradiol 2005, 26 (4) 973-980
<http://www.ajnr.org/content/26/4/973>

Imaging of Intra-neural Edema by Using Gadolinium-Enhanced MR Imaging: Experimental Compression Injury

Shigeru Kobayashi, Adam Meir, Hisatoshi Baba, Kenzo Uchida, and Katsuhiko Hayakawa

BACKGROUND AND PURPOSE: Compressive and entrapment neuropathies are diseases frequently observed on routine clinical examination. A definitive diagnosis based on clinical symptoms and neurologic findings alone is difficult in many cases, however, and electrophysiologic measurement is used as a supplementary diagnostic method. In this study, we examined to use protein tracers (Evans blue albumin or horseradish peroxidase) and gadolinium-enhanced MR imaging to determine the changes of blood-nerve barrier permeability in compressive neuropathies.

METHODS: In dogs, the median nerve was compressed for 1 hour by using five kinds of clips with various strengths (7.5–90-g force). After clip removal, the combined tracers of Evans blue albumin and gadolinium or horseradish peroxidase was administered intravenously as a tracer. After the animals were euthenized, we compared gadolinium-enhanced MR images with Evans blue albumin distribution in the nerve under fluorescence microscopy. The horseradish peroxidase-injected specimens were observed by transmission electron microscopy.

RESULTS: On enhanced MR imaging, intra-neural enhancement was caused by 60- and 90-g-force compression after 1 hour. Marked extravasation of protein tracers in the nerve occurred where there was compression by 60- and 90-g-force compression, and capillaries in the nerve showed the opening of tight junction and an increase of vesicular transport under the electron microscopy. This situation indicated breakdown of the blood-nerve barrier, with consequent edema formation and was seen as enhancement on MR imaging.

CONCLUSION: Gadolinium-enhanced MR imaging can detect morphologic and functional changes of blood-nerve barrier in the nerve induced by mechanical compression.

It is generally considered that the genesis of neuropathy associated with compressive and entrapment neuropathies—such as carpal tunnel syndrome, cubital tunnel syndrome, and trauma—may result from both mechanical compression and vascular problems. The blood-nerve barrier has analogous functions to the blood-brain barrier, but both restraint to the penetration of materials and selectivity are less in the blood-nerve barrier than in the blood-brain barrier. The internal milieu of peripheral nerve fascicles is nor-

mally controlled by combined barrier action of the endoneurial blood vessels (1–5) and perineurium (6–13). Peripheral nerves may be compressed acutely or may be subjected to chronic lesions. The primary cause of compressive neuropathy is likely the mechanical compression of the nerve due to osseous, cartilaginous, muscle, or fibrous tissues based on the degenerative disease and trauma. Mechanical compression also may change the intra-neural circulation (14–18). Intra-neural edema may be formed in nerves as a result of compression injury (19–23).

MR imaging of peripheral nerves recently relies on the use of T2-weighted images (24–27). When peripheral nerves are damaged, they may become hyperintense on T2-weighted images. It is difficult, however, to examine nerve signal intensity change should be quantified. Jarvik et al had reported that nerve signal intensity evaluation relies on the visual inspection of an experienced observer (26). Gadolinium diethylene triamine pentaacetic acid (Gd-DTPA), a paramagnetic contrast agent, is used to investigate a variety of disorders. It thus would seem possible that,

Received August 4, 2004; accepted November 10.

From the Physiology Laboratory of Oxford University (S.K., A.M.), Oxford, United Kingdom; the Department of Orthopedics and Rehabilitation Medicine (S.K., H.B., K.U.), Fukui University School of Medicine, Fukui, Japan; and the Department of Radiology and Orthopedics (K.H.), Aiko Orthopedic Hospital, Aichi, Japan.

Address reprints requests and correspondence to Shigeru Kobayashi, MD., PhD., Department of Orthopedics and Rehabilitation Medicine, Fukui University School of Medicine, Shimoaizuki 23, Matsuoka, Fukui, 910-1193, Japan.

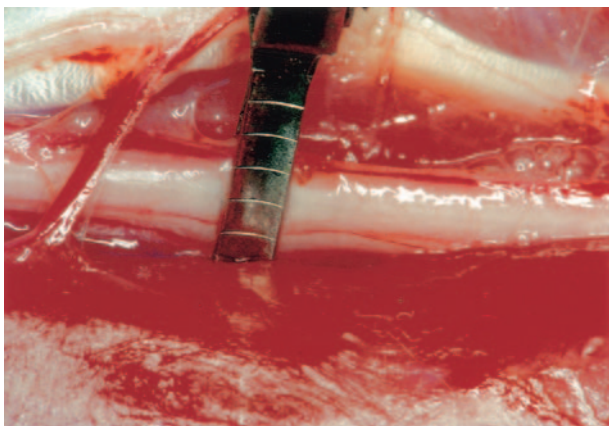


Fig 1. Clamping of the median nerve. The median nerve was clamped with a clip for microvascular suturing at the proximal portion of the carpal tunnel. The compression force used in this study was about 60 g, and the nerve was compressed continuously for 1 hour.

with sufficient spatial and temporal resolution, the enhancement pattern at MR imaging may give us an idea about the status of blood-nerve barrier to peripheral nerve (28). If the technique devised to visualize the status of blood-nerve barrier to the nerve bundle should prove successful, this technique could serve as a new diagnostic tool with which to detect compressive and entrapment neuropathies. The aim of the present experimental investigation is to study the status of the blood-nerve barrier in the median nerve under normal condition and acute compression in adult dogs by using protein tracers (Evans blue albumin or horseradish peroxidase) and gadolinium-enhanced MR imaging to determine the pathologic focus for the MR imaging findings related to compressive and entrapment neuropathies.

Methods

The experiment was carried out under the control of the local animal ethics committee in accordance with the guidelines on animal experiments in our university, Japanese government animal protection and management law, and Japanese government notification on feeding and safekeeping of animals. Twenty-five dogs, weighing 10–15 kg, were anesthetized with intramuscular injection of 3 mL of Ketalar (Ketamine 50 mg/mL; Waner-Lumbert, Morris Plains, NJ) and ventilated a respirator under general anesthesia (O_2 , 3 mL/min; N_2O , 3 mL/min; Halothane, 1.5 mL/min). A common iliac arterial catheter and rectal temperature probe were placed to monitor blood pressure and temperature. Animals were thus maintained at constant physiologic levels. Each animal was placed in the prone position on a frame, the skin of the palmar side at one-third distal of the forearm was cut, and the median nerve was exposed and entrapped with a clip for microvascular suturing. Before by using the clip, clipping power was measured by a tension device of Instron type (AGH-2000B, Simazu Co., Kyoto, Japan) (21). The left median nerve was compressed by using a vascular clip (Kouno Co., Chiba, Japan) at 90-, 60-, 30-, 15-, or 7.5-g force for 1 hour in eight animals each (Fig 1). The contralateral median nerve was only exposed and used as control.

Three tracer techniques were used to investigate the status of the barrier function. The tracers were Evans blue albumin (5 mL/kg; molecular weight \sim 59,000; Sigma Chemical Co., St.

Louis, MO), horseradish peroxidase (Type II, 200 mg/kg; molecular weight \sim 43,000; Sigma Chemical Co.) and Gd-DTPA (0.1 mmol/kg; molecular weight \sim 743; Schering Co., Berlin, Germany). Evans blue albumin was prepared by mixing 5% bovine albumin (Wako Chemical Co., Osaka, Japan) with 1% Evans blue (Sigma Chemical Co.). Horseradish peroxidase of the protein tracer was dissolved in Ringer-Hartmann solution. Gd-DTPA was simultaneously injected with Evans blue albumin ($n = 25$). After the clamp was released, the tracers were given intravenously. The protein tracers were allowed to circulate for 1 hour before the nerves were removed. The combined tracers of Gd-DTPA and Evans blue albumin were allowed to circulate for 10 minutes before a mass of forearm, including the median nerve, was removed.

Preparation for Fluorescence Microscopic Study

The specimens injected with Evans blue albumin were fixed in 4% paraformaldehyde for 24 hours. Transverse sections of the nerve 20 μ m thick were mounted in 50% aqueous glycerin and examined under a fluorescence microscope at 380 $m\mu$ W. Evans blue albumin emits a bright red fluorescence in clear contrast to the green fluorescence of the nerve tissue.

Preparation for Transmission Electron Microscopic Study

The specimens ($n = 15$) injected with horseradish peroxidase were fixed by intraaortal perfusion with 4% paraformaldehyde and 1% glutaraldehyde in 0.15 mol/L cacodylate buffer, pH 7.2 at 20°C. After 15 minutes, the median nerve were carefully removed and fixed by immersion in the same fixative for 24 hours at 4°C. After fixation, the blocks of the tissue were washed for 3 days in saccharin and then sliced to approximately 50- μ m thickness by using a cryostat. The sections were incubated for 15 minutes at room temperature in 0.05 mol/L Tris-HCl buffer, at pH 7.6, containing 4.0 mg of 3–3'-diaminobenzidine (Sigma Chemical Co.) per 10 mL of buffer and a final concentration of 0.01% hydrogen peroxide. The specimens were then rinsed in 0.05 mol/L Tris-HCl buffer, postfixed at room temperature for 3 hours in 2% OsO₄ in 0.1 mol/L sodium cacodylate buffer, impregnated with 2% uranyl acetate, dehydrated in graded ethanols, and embedded in epoxy resin. For light microscopy, 1–3- μ m-thick toluidine blue-stained sections were used. For electron microscopy, ultrathin sections contrasted with uranyl acetate and lead citrate were examined under JSM-2000FX electron microscope (Hitachi Co., Tokyo, Japan). The reaction products of horseradish peroxidase were visualized as electron-attenuated black under the electron microscope.

Preparation for Gadolinium-Enhanced Imaging

The specimens injected with Gd-DTPA and Evans blue albumin were fixed by intraaortal perfusion with 4% paraformaldehyde, and a mass of the forearm including the median nerve was removed. MR studies were performed on a 0.3-T permanent magnet (Magnetom; Hitachi MRP7000) by using 16.5-cm-diameter planar circular surface coil operating in the receive mode. A 50-cm body coil served as the transmitter. Sequences included axial T1-weighted spin-echo (SE) images, 600/25 (TR/TE), under conditions of 4-mm section thickness, 50% interslice gap, 256 \times 256 matrix, and 4 excitations. After gadolinium injection, the brightness in the nerve seen on T1-weighted images indicated accumulation of gadolinium in the endoneurial space. Therefore, the intraneural edema can be delineated with enhanced MR imaging; however, it is difficult to examine nerve signal intensity change should be quantified by using T2-weighted images. Finally, we compared gadolinium-enhanced MR images with Evans blue albumin distribution in the nerve under a fluorescence microscope.

Results

Barrier System of the Peripheral Nerve

The median nerve exhibited moderate signal intensities and the signal intensity was similar to that of muscle in normal conditions. There was no extravasation of Evans blue albumin in the nerve under the fluorescence microscope. That is to say, Gd-DTPA does not leak into the endoneurial space of the nerve (Fig 2A). Fluorescence microscopic study indicated that Evans blue albumin mixed with Gd-DTPA could not pass from the blood vessels into the endoneurial space of the nerve (Fig 2B).

By electron microscope, capillaries of the median nerve were shown to have an inner diameter of $\sim 10 \mu\text{m}$. The arterioles, venules, and capillaries in the endoneurial space of the median nerve are all continuous type, and their endothelial cells are linked by tight junctions showing the existence of a blood-nerve barrier. In fact, horseradish peroxidase did not appear in the endoneurial space when it was injected intravenously (Fig 3A). Few horseradish peroxidase-labeled vesicles related to transcellular transport were detected in the endothelial cells of capillaries in the median nerve, and there was no extravasation of horseradish peroxidase under normal condition (Fig 3B).

Blood Permeability under Compression

There was no extravasation of protein tracers and no enhancement after compression at 7.5- and 15-g force. After compression at 30-g force, there was congestion of Evans blue albumin in the intraneural vessels, and in three of five nerves (60%) was seen the limited extravasation of Evans blue albumin around the vessels (Fig 2C). The median nerve, however, did not show any enhancement by gadolinium (Fig 2D). Gadolinium enhancement in the median nerve was induced by 90- and 60-g-force compression after 1 hour. The enhancement was seen diffusely throughout the nerve at the compressed zone (Fig 2E). Evans blue albumin tracer study showed the same distribution as the Gd-DTPA tracer under fluorescence microscope and indicated breakdown of the blood-nerve barrier, with consequent edema formation in the median nerve. The red fluorescence of Evans blue albumin tracer was seen outside the endoneurial microvessels and diffusely throughout the endoneurial space at the compressed zone (Fig 2F; Table 1).

Horseradish peroxidase had the same distribution as the Evans blue albumin tracer under the light and electron microscope. Under the electron microscope, the extravasation of horseradish peroxidase tracer was observed in endoneurial spaces between the nerve fibers, especially perivascular spaces. The tight junctions of the endothelial cells of the capillary were open, and the dark-stained horseradish peroxidase product extravasated through the junctions into the endoneurial space (Fig 4A). Pinocytotic vesicles appeared to carry the product away from the capillary. This increased paracellular and transcellular transport of the tracer indicates breakdown of the blood-

nerve barrier, leading to edema formation in the nerve (Fig 4B).

Discussion

In 1941, Manery and Bale reported the occurrence of blood-nerve barrier in the peripheral nerve similar to the blood-brain barrier in the central nervous system (29). The existence of blood-nerve barrier was confirmed by experiment by Waksman in 1961 (30), who studied the distribution in the peripheral nervous system of intravenously injected dyes, proteins, and diphtheria toxins and toxoids. Since the development of the electron microscope, the structural and physiologic aspects of the permeability of blood capillaries have been studied extensively. Bennett et al have demonstrated the morphologic classification of capillaries based on the presence or absence of continuous basement membrane, the nature of the endothelial cell, and the presence or absence of a complete investment of pericytes (31). It is suggested that these structural features of the capillary may be relevant to problems related to the exchange of materials between blood plasma and parenchymal cells. In general, true capillaries are classified into three types: continuous, fenestrated, and discontinuous. Continuous capillaries distinguish brain type from muscle type (Fig 5). Capillaries of brain type are mainly located in the central and peripheral nervous systems where the blood-brain (nerve) barrier is present. Thereafter, several workers have demonstrated deep involvement of breakage of this blood-nerve barrier in intraneural edema that induces neural dysfunction by basic studies. In general, the peripheral nerve has the perineurium as a diffusion barrier and the blood-nerve barrier also exists in the endothelial cells of the endoneurial microvessels. These barriers of the peripheral nerve protect and maintain the nerve fibers in a constant environment (Fig 6). The blood-nerve barrier of endothelial blood vessels consists of tight junctions (zonulae occludentes) between adjacent endothelial cells and a very small number of endothelial vesicles. When the barrier to protein is altered, with consequent vasogenic edema, one or both these factors may be modified to serve as leakage routes from the lumen to the tissue front.

In this study, examination was made of blood-nerve barrier function by using protein tracers of Evans blue albumin and horseradish peroxidase. Albumin is about 4.2 nm in diameter and has a molecular weight of 59,000; horseradish peroxidase is about 4 nm in diameter and has a molecular weight of 43,000. The capillaries in the endoneurial space of the median nerve are all of the continuous type capillaries. Their endothelial cells are thus linked with tight junctions showing the existence of a blood-nerve barrier. Tight junctions normally allow molecules no larger than 2–3 nm to pass freely into the extravascular (endoneurial) space. Pinocytotic vesicles related to transport of nutrients and waste matter are a few in endothelial cells of a capillary on peripheral nerves. Pinocytotic vesicles range from 60 to 100 nm in diameter. The median

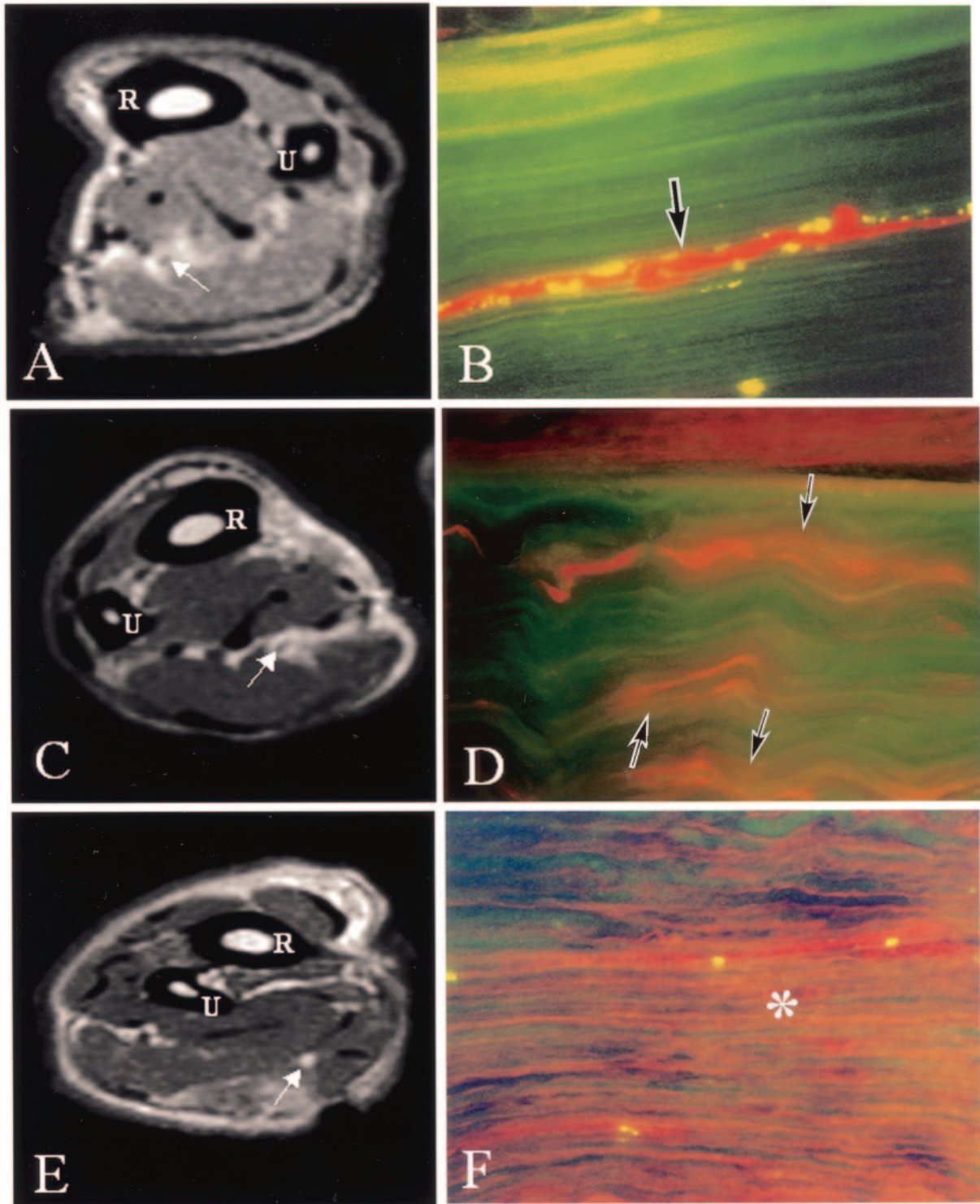


FIG 2. Comparison between enhanced MR imaging and fluorescent micrograph of the median nerve.

A and B, No enhancement of a healthy median nerve was found on a gadolinium-enhanced MR image (T1-weighted SE image, 600/25 [TR/TE]). The median nerve showed moderate signal intensities and the signal intensity was similar to that of muscle in normal conditions (*A*, arrow). Evans blue albumin was limited inside the blood vessels (*B*, arrow), and the blood-nerve barrier was maintained as seen under fluorescent microscopy.

C and D, After compression with a 30-g force, no enhancement of median nerve was found on gadolinium-enhanced MR image (T1-weighted SE image, 600/25 [TR/TE]; *C*, arrow); however, there was seen the limited extravasation of protein tracers around intraneural blood vessels (*D*, arrows).

E and F, Clear enhancement was seen inside the nerve compressed by a 60-g-force clip as seen on gadolinium-enhanced MR image (T1-weighted SE image, 600/25 [TR/TE]; *E*, arrow). In the nerve, where enhancement was found on MR imaging, Evans blue albumin emits a bright red fluorescence, which leaked outside the blood vessels, and intraneural edema was seen under a fluorescent microscope (*F*, asterisk). R, radius; U, ulna.

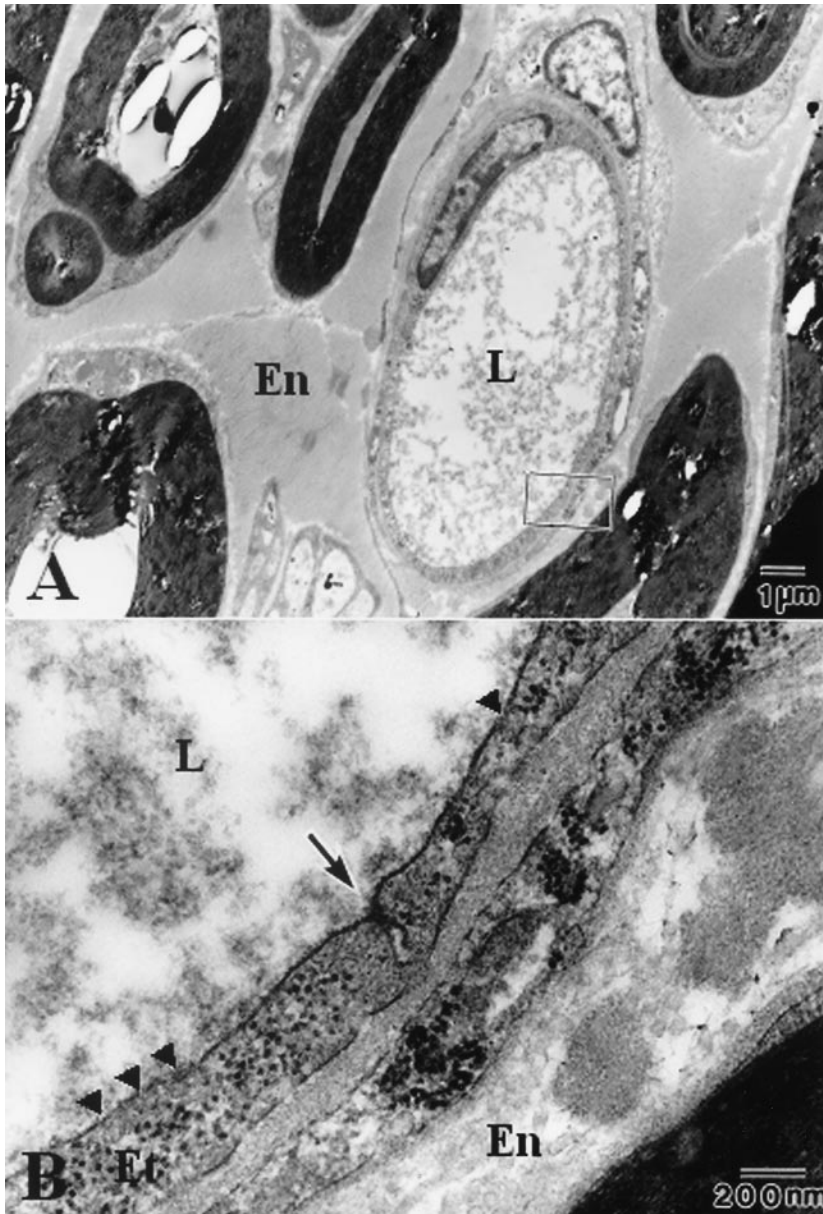


FIG 3. Electron micrographs of the unaffected median nerve after intravenous injection of horseradish peroxidase.

A, In the normal median nerve without compression, electron-attenuated horseradish peroxidase was found in capillary lumen, but no leakage into the endoneurial space was observed.

B, There are a very small number of pinocytotic vesicles in the endothelium (arrowheads). The tight junction (arrow) among endothelial cells was closed, and the blood-nerve barrier was maintained (A, $\times 5,000$; B, $\times 40,000$). En, endoneurial space, E, endothelium; L, capillary lumen.

Comparison of fluorescent microscopy findings and gadolinium-enhanced MR imaging

Compression power	Compression power					
	Control	7.5 gf	15 gf	30 gf	60 gf	90 gf
Tracer	-	-	-	-	++	++
EBA+Gd-DTPA	-	-	-	+	++	++
(n = 30)	-	-	-	-	++	++
	-	-	-	+	++	++
HRP	-	-	-	-	++	++
(n = 18)	-	-	-	+	++	++

Note.—After 1-hour compression, the protein tracer (EBA, HRP) and Gd-DTPA were allowed to circulate for 1 hour. -, indicates no extravasation of protein tracers and no enhancement of median nerve; +, limited extravasation of protein tracers around intraneural blood vessels and no enhancement of median nerve; ++, marked extravasation of protein tracers in the nerve and enhancement of median nerve; N, number of animals; gf, gram force.

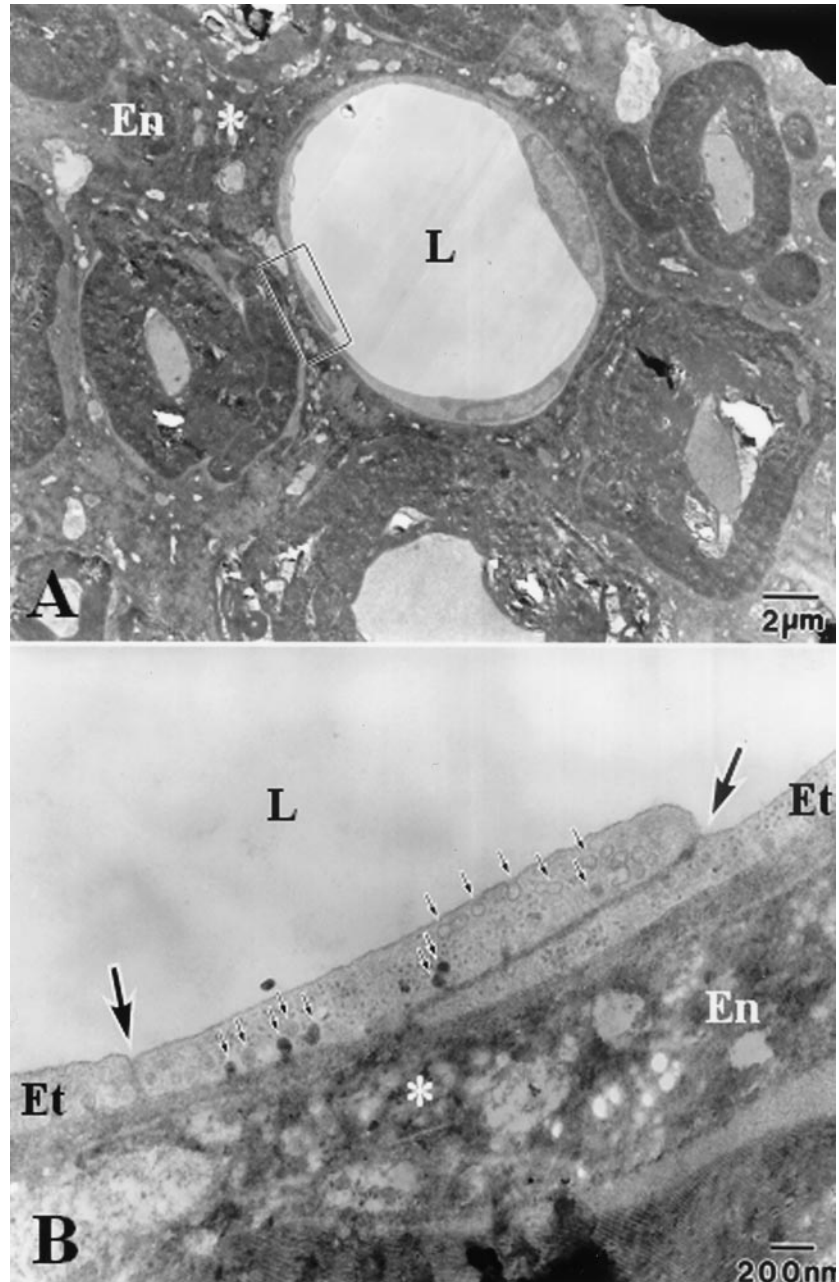
nerve did not show any enhancement in normal conditions. That is to say, Gd-DTPA does not leak into the endoneurial space of the nerve. Fluorescence microscopic study indicated that Evans blue albumin mixed with Gd-DTPA could not pass from the blood vessels into the endoneurial space of the nerve.

Olsson classified edema of peripheral nerve based on the presence or absence of increased vascular permeability to protein into vasogenic edema and nonvasogenic edema and the latter into extracellular type and intracellular type depending on the site of water accumulation (2). In general, intraneural edema caused by mechanical compression is a vasogenic edema induced by congesting venous blood flow, as suggested by Sunderland (32), and develops because of increased permeability of capillaries in the endoneurial space, that is, leaking of water and macromolecular substances such as protein from blood vessels into endoneurial space. In turn, leakage of

FIG 4. Electron micrographs of the affected median nerve after intravenous injection of horseradish peroxidase.

A, After 1 hour of perfusion, the dark reaction product of horseradish peroxidase leaks out of capillary under compression (asterisk).

B, Horseradish peroxidase leaked into the endoneurial space from capillary lumen owing to expansion of the tight junction (large arrow) and increased transcellular transport by pinocytotic vesicles (small arrow). The dark reaction products of horseradish peroxidase pass through from capillary lumen to endoneurial space. Occurrence of intraneural edema was shown (asterisk). The lumen has been cleared of horseradish peroxidase by perfusion fixation (A, $\times 3,000$; B, $\times 25,000$). En, endoneurial space; Et, endothelium; L, capillary lumen.



edematous fluid into the endoneurial space elevates endoneurial pressure (33) and appears to induce demyelination that is deeply involved in onset of neuropathy. Rydevik et al examined (34) the possibility of analyzing the intraneural blood flow of epineural vessels and endoneurial capillaries during and after localized compression by using intravital microscopic techniques. When a nerve was compressed experimentally, external pressures of 20–30 mmHg induced a retardation of venular blood flow in the epineurium. Compression at 60–80 mmHg induced complete circulatory arrest in compressed nerve segments. They also showed the leakage of Evans blue albumin from intraneural microvessels after acute compression (20). This resulted in edema formation in the endoneurial space occurred at the edges of compressed

segments in all fascicles as nerve were compressed at 200 and 400 mmHg for 2 hours. In the present study, the strength of the spring clips used for nerve compression was determined with an Instron-type tensile tester. On the assumption that the strength of the springs follows the law of Young, the weight required to open a clip 2 mm was determined, and five types of clips with different compression forces were prepared by adjusting the strength of the spring. The compression force required to open a clip 2 mm was determined because the longitudinal diameter of the median nerve is 3.5 ± 0.3 mm. The pressure actually applied to the nerve can be calculated in mmHg from the following equation: $1033.6\text{-g force/cm}^2 = 760$ mmHg. The area (cm^2) of a clip in contact with the nerve is 0.2 cm (width of a clip) $\times 0.35$ cm (longitudi-

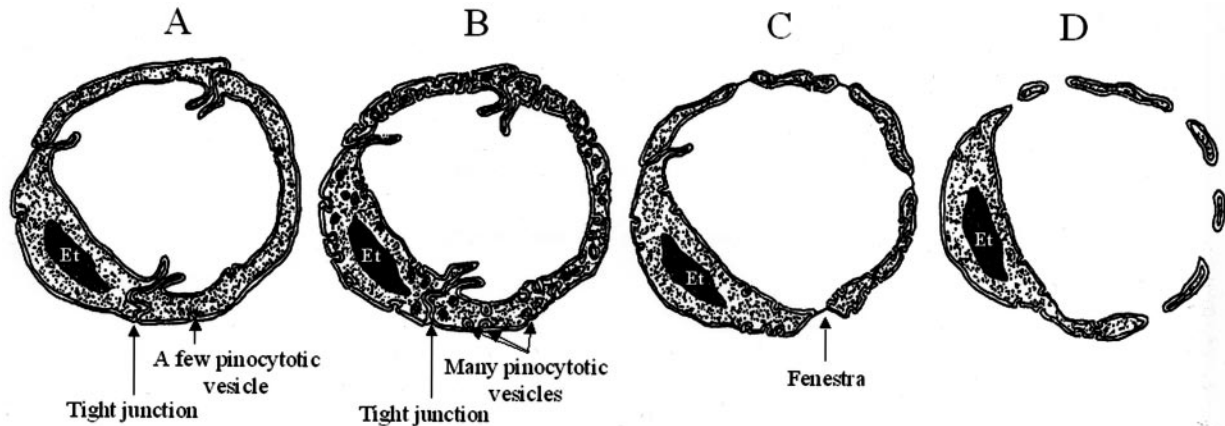


FIG 5. Classification of the true capillary.

A, Brain type of continuous capillary. In morphologic features, the blood-brain (nerve) barrier of endothelial blood vessels consists of tight junction (zonulae occludentes) between adjacent endothelial cells and a very small number of pinocytotic vesicles. This capillary is mainly located in the central and peripheral nerve.

B, Muscle type of continuous capillary. In morphologic features, their endothelial cells are linked with tight junction; however, pinocytotic vesicles related to transport of nutrients and waste matter are much more abundant in endothelial cells of a capillary on muscle than capillary of brain type.

C, Fenestrated capillary. This capillary has a fenestration with a diaphragm in an endothelial cell and is mainly located in stomach, colon, and kidney.

D, Discontinuous capillary (sinusoid). Between the endothelial cells are large gaps, which permit a direct continuity of access of blood plasma from the lumen to the extracellular space. This capillary is mainly located in liver, spleen, hypophysis cerebre, and bone marrow. Et, vascular endothelium.

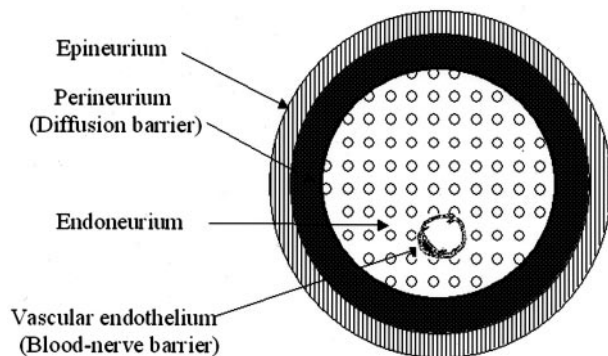


FIG 6. Barrier systems of peripheral nerve. Normally, the internal milieu of peripheral nerve fascicles is controlled by combined barrier action of the endothelial blood vessels and perineurium.

dinal diameter of nerve) = 0.07 cm^2). Therefore, 1 g of force represents about 8.75 mmHg of pressure. In the present study, the vascular permeability of the median nerve was appeared by compression at 30-g force (about 263 mmHg) or higher after 1 hour. In patients with entrapment neuropathy, however, the nerve bundle environment differs markedly from that in this animal model. Neither the duration of nerve compression nor the pressure on the nerve bundle is the same. It is very difficult, however, to distinguish acute from chronic compression to the nerve as the cause of entrapment neuropathy. For example, the median nerve of the carpal tunnel always moves with movement of the wrist, and the dynamic limit is dependent on the positional relationship between the nerve and the surrounding tissues. Thus, when narrowing of the carpal canal is caused, movement of the nerve along with movement of the wrist becomes limited, and consequently compression and traction

on the nerve cause neuropathy. In fact, symptoms are frequently alleviated by rest in patients with carpal tunnel syndrome and are intensified by application of acute compression to the nerve during wrist flexion test (Phalen's test). We believe that chronic compression is the result of repeated episodes of mild acute compression.

In the median nerve compression model that we prepared in the present study, on enhanced MR imaging enhancement in the nerve was induced by 60- and 90-g-force compression after 1 hour. The enhancement of Gd-DTPA under MR imaging was seen diffusely throughout the nerve at the compressed zone. The tracer study of Evans blue albumin showed the same distribution as the Gd-DTPA tracer under fluorescence microscope and indicated breakdown of the blood-nerve barrier, with consequent edema formation in the median nerve. In addition, electron microscopic examination after intravenous injection of horseradish peroxidase showed occurrence of breakage of this blood-nerve barrier via increased paracellular transport due to expansion of tight junction between vascular endothelial cells, and increased transcellular transport due to pinocytotic vesicles were demonstrated. Namely, gadolinium seemed to leak outside the blood vessels via this route in the nerve of which blood-nerve barrier was broken by compression and this was reflected as high intensity on gadolinium-enhanced MR imaging. The results of the present experimental studies demonstrated that intraneural edema could be visualized by comparing T1-weighted image before and after administration of contrast medium. Although this study used an acute model, the affected nerves will show enhancement on MR imaging at the site of the compression in entrap-

ment neuropathy, such as carpal tunnel syndrome and trauma. In this respect, gadolinium-enhanced MR imaging might be available to evaluate the blood-nerve barrier permeability changes in compressive and entrapment neuropathies.

Conclusion

MR imaging may demonstrate intraneural enhancement at the site of nerve entrapment where intraneural edema resulted from an increase in the vascular permeability of the endoneurium. We therefore may safely say that enhanced MR imaging might be available to evaluate the blood-nerve barrier permeability changes in compressive and entrapment neuropathies.

Acknowledgments

The submitted manuscript does not contain information about medical devices or drugs. No benefits in any form have been received or will be received from a commercial party related directly or indirectly to the subject of this article. Mr. Takashi Nakane provided expert help with the MR imaging study. Mr. Naruo Yamashita provided expert help with the photography. The authors would like to thank Ms. Mika Osaki and Yukiko Horiuchi for their dedicated assistance in this study.

References

1. Olsson Y. Studies on vascular permeability of the peripheral nerves: distribution of circulating fluorescent serum albumin in normal, crushed and sections rat sciatic nerve. *Acta Neuropathol* 1966;7:1-15
2. Olsson Y. Topographical differences in the vascular permeability of the peripheral nervous system. *Acta Neuropathol* 1968;10:26-33
3. Reese TS, Olsson Y. Fine structural localization of a blood-nerve barrier in the mice. *J Neuropathol Exp Neurol* 1970;29:123-128
4. Oldfors A, Sourander P. Barriers of peripheral nerve towards exogenous peroxidase normal and protein deprived rats. *Acta Neuropathol* 1978;43:129-134
5. Olsson Y. Vascular permeability in the peripheral nervous system. In: Dyck PJ, Thomas PK, Lambert EH, Bunge R, eds. *Peripheral neuropathy*. 2nd ed. Philadelphia: WB Saunders;1989:579-597
6. Wagger JD, Bunn SM, Begg J. The diffusion of ferritin within the peripheral nerve sheath: an electron microscopy study. *J Neuropathol Exp Neurol* 1965;24:430-443
7. Kristensson K, Olsson Y. The perineurium as a diffusion barrier to protein tracers: differences between mature and immature animals. *Acta Neuropathol* 1971;17:127-138
8. Olsson Y. Studies on vascular permeability in peripheral nervous. IV. Distribution of intravenously injected protein tracers in the peripheral nerve system of various species. *Acta Neuropathol (Berl)* 1971;17:114-126
9. Olsson Y, Reese TS. Permeability of vasa nervosa and perineurium in mice sciatic nerve studied by fluorescence and electron microscopy. *J Neuropathol Exp Neurol* 1971;30:105-119
10. Lundborg G, Nordborg C, Rydevik B, Olsson Y. The effect of ischemia on the permeability of the perineurium to protein tracers in rabbit tibial nerve. *Acta Neurol Scandinav* 1973;49:287-294
11. Olsson Y, Kristensson K. The perineurium as a diffusion barrier to protein tracers following trauma to nerves. *Acta Neuropathol* 1973;23:105-111
12. Sima A, Sourander P. The effect of perinatal undernutrition on perineurial diffusion barrier to exogenous protein: an experimental study on rat sciatic nerve. *Acta Neuropathol* 1973;24:263-272
13. Soderfeldt B. The perineurium as a diffusion barrier to protein tracers in human peripheral nerve. *Acta Neuropathol* 1973;25:120-126
14. Yoshizawa H, Kobayashi S, Kubota K. Effect of compression on intraradicular blood flow in dogs. *Spine* 1989;14:1220-1225
15. Kobayashi S, Yoshizawa H, Nakai S. Experimental study on the dynamics of lumbosacral nerve root circulation. *Spine* 2000;25:298-305
16. Kobayashi S, Shizu N, Suzuki Y, et al. Changes of nerve root motion and intraradicular blood flow during an intraoperative SLR test. *Spine* 2003;28:1427-1434
17. Kobayashi S, Suzuki Y, Asai T, et al. Changes of nerve root motion and intraradicular blood flow during an intraoperative femoral nerve stretch test. *J Neurosurg (Spine 3)* 2003;28:298-305
18. Lundborg G. Ischemic nerve injury. experimental studies on intraneurial microvascular pathophysiology and nerve function in a limb subjected to temporary circulatory arrest. *Scand J Plast Reconstr* 1970;6(suppl):11-47
19. Lundborg G. Structure and function of the intraneurial microvessels as related to trauma, edema formation, and nerve function. *J Bone Joint Surg* 1975;57A:938-948
20. Rydevik B, Lundborg G. Permeability of intraneurial microvessels and perineurium following acute, graded experimental nerve compression. *Scand J Plast Reconstr Surg* 1977;11:179-187
21. Kobayashi S, Yoshizawa H. Effect of mechanical compression on the vascular permeability of the dorsal root ganglion. *J Orthop Res* 2002;20:730-739
22. Kobayashi S, Yoshizawa H, Yamada S. Pathology of lumbar nerve root compression. Part 1. Intraradicular inflammatory changes induced by mechanical compression. *J Orthop Res* 2004;22:170-179
23. Kobayashi S, Yoshizawa H, Yamada S. Pathology of lumbar nerve root compression. Part 2. Morphological and immunohistochemical changes of dorsal root ganglion. *J Orthop Res* 2004;22:180-188
24. Cudlip SA, Howe FA, Griffiths JR, et al. Magnetic resonance neurography of peripheral nerve following experimental crush injury, and correlation with functional deficit. *J Neurosurg* 2002;96:755-759
25. Cudlip SA, Howe FA, Clifton A, et al. Magnetic resonance neurography studies of the median nerve before and after carpal tunnel decompression. *J Neurosurg* 2002;96:1046-1051
26. Jarvik JG, Yuen E, Kliot M. Diagnosis of carpal tunnel syndrome. electrodiagnostic and MR imaging evaluation. *Neuroimaging Clin N Am* 2004;14:93-102
27. Bordalo-Rodrigues M, Amin P, Rosenberg ZS. MR imaging of common entrapment neuropathies at the wrist. *Magn Reson Imaging Clin N Am* 2004;12:265-279
28. Sugimoto H, Miyaji N, Ohsawa T. Carpal tunnel syndrome: evaluation of median nerve circulation with dynamic contrast-enhanced MR imaging. *Radiology* 1994;190:459-466
29. Manery JF, Bale WF. The penetration of radioactive sodium and phosphorus into the extra- and intracellular phases of tissues. *Am J Physiol* 1941;132:215-231
30. Waksman BH. Experimental study of diphtheritic polyneuritis in the rabbit and guinea pig: the blood-nerve barrier in rabbit. *J Neuropathol Exp Neurol* 1961;20:35-77
31. Bennett HS, Luft JH, Hampton JC. Morphological classification of vertebrate blood capillaries. *Am J Physiol* 1959;196:381-390
32. Sunderland S. The nerve lesion in the carpal tunnel syndrome. *J Neurol Neurosurg Psychiatry* 1976;39:615-626
33. Myers RR, Powel HC. Endoneurial fluid pressure in peripheral neuropathies. In: Hargens AR, ed. *Tissue Fluid Pressure and Compression*. Baltimore: Williams & Wilkins;1981:193-207
34. Rydevik B, Lundborg G, Bagge U. Effects of graded compression on intraneurial blood flow. *J Hand Surg* 1981;6:3-12